

Study on stainless steel 316L coatings sprayed by high pressure HVOF

B. Sun and H. Fukanuma, Saitama/J

The conventional high-velocity oxy-fuel (HVOF) process has characteristics of high flame velocity and moderate temperature, and is widely used to deposit cements, metals and alloys coatings such as WC-Co, nickel and stainless steel. In this paper, a high pressure HVOF system with combustion chamber pressure up to 3.0MPa, and with characteristics of higher flame velocity and lower temperature was developed.

In-flight particle velocity was measured using the DPV-2000 system at combustion chamber pressures from 1.0 to 3.0MPa, and stainless steel 316L powder was deposited at a combustion chamber pressure of 3.0MPa. The influence of spray conditions on the coating microstructure, deposition efficiency and micro-hardness were investigated. It was shown that the combustion chamber pressure has significant influence on particle velocity. Dense coatings composed of unmolten or partially molten particles could be deposited by varying the spray parameters. In the experiment, deposition efficiency up to 90% was achieved at the optimized spray conditions.

1 Introduction

In the high velocity oxygen-fuel (HVOF) process, liquid or gaseous fuel and oxygen are injected into a confined combustion chamber, then ignited and burned to produce heat and pressure. The velocity of combustion products is accelerated by passing through a convergent-divergent nozzle or a convergent nozzle. The powder feedstocks are injected into the combustion flame jet and subsequently are heated and accelerated through heat and momentum transfer from the flame jet. Compared to other spray processes the HVOF process has special features of higher particle velocity and lower particle temperature, which give it a superior ability in producing denser, more wear-resistant and more corrosion-resistant coatings. It has been widely used to deposit carbide-based cements, metals and alloy coatings such as WC-Co, nickel and stainless steel materials [1, 2]. However, as a spray process employed in atmosphere the ambient air entrainment into the flame jet is inevitable which usually causes in-flight particle oxidation [3]. The oxidation may undesirably affect phase composition, microstructure and performance of the deposited coatings, especially for materials or applications sensitive to oxidation [4, 5]. In addition, during the HVOF spraying WC-Co cermet process, it is commonly accompanied by the decarburization of tungsten carbide (WC), which results in the formation of dicarbide (W_2C) and metallic tungsten (W) [6]. The reduction of WC in the coating after the spraying will degrade the wear resistance of the coatings [7, 8].

To improve the abovementioned shortcomings of the HVOF process, A. Dolatabadi and Pershin designed a protective shroud attaching to the end of the HVOF nozzle, which can prevent ambient air from penetrating the spray flame jet. The experiment results showed that the protective shroud brings not only a significant reduction in in-flight particle oxidation but also a more uniform particle velocity and temperature distribution [9]. In consideration of the characteristics of the cold spray process, recently other approaches named warm spray or low temperature oxy-fuel (LTOF) were reported [10, 11]. By injecting additional nitrogen gas or water into the

combustion chamber of the conventional HVOF torch, the flame jet temperature can be controlled at lower range and thereby the particles can be heated to a temperature below the melting point but higher than that of cold spray. The warm spray or LTOF processes covered the existing gap between the conventional HVOF and cold spraying, and provided potential applications to produce coatings which are difficult to be deposited by the cold spray process, such as WC-Co, titanium alloys and some superalloy coatings [12, 13].

In the cold spray process the coatings are formed by the high velocity impact of solid powders. Many researchers have argued that only the spray particles at a velocity higher than the critical velocity can achieve deposition, and higher particle velocity enhances the deformation, adhesion and cohesion of the particles [14, 15, 16]. As for the warm spray and LTOF spray, the process operated in the temperature range between HVOF spraying and cold spraying, the powder materials remain unmolten during spraying. It can be reasonably supposed that higher velocity particles will form denser coatings with high performance. However, there is no clear evidence showing that higher particle velocity is obtained in the warm spray or LTOF spray process.

In this paper, an approach aimed to accelerate the spray particle to higher velocity in partially molten or un-molten state was proposed. A high pressure HVOF system with combustion chamber pressure up to 3.0MPa, and with characteristics of higher flame velocity and lower temperature was developed. Stainless steel 316L particle was used as the spray material. The influence of spray parameters on the particle velocity, deposition efficiency, microstructure and microhardness of the coating were investigated.

2 Experiment equipment and methods

2.1 High pressure HVOF equipment

In the one-dimensional two-phase flow (gas and particles) the acceleration of the particle velocity can be equated to the drag force on the particle:

$$\frac{dV_p}{dt} = V_p \frac{dV_p}{dx} = \frac{3}{4} C_D (V_g - V_p) |V_f - V_p| \frac{\rho_g}{\rho_p d_p} \quad (\text{Eq. 1})$$

where, V_p : particle velocity, V_g : gas velocity, C_D : drag coefficient, ρ_p : particle density, ρ_g : gas density

Therefore, for a given type of spray process and spray powders, the particle velocity is determined by the gas velocity, density and the acceleration distance in the barrel. Higher gas velocity and density, as well as a longer barrel will contribute to accelerate the spray particle to higher velocity.

Considering the HVOF process as simplified one-dimensional isentropic supersonic flow, gas velocity within the convergent-divergent nozzle is a function of only the stagnation gas temperature and the nozzle geometry (Eq.2, Eq.3). Gas pressure does not affect the gas velocity. However, examination of Eq.1, Eq.4, Eq.5 and Eq.6 shows that the drag force on the particle is linearly dependent on the stagnation gas pressure. Therefore, gas pressure is a key factor in determining the particle velocity.

$$\frac{T_0}{T} = 1 + \frac{k-1}{2} M^2 \quad (\text{Eq. 2})$$

$$\frac{A}{A^*} = \frac{1}{M} \left[\left(\frac{2}{k+1} \right) \left(1 + \frac{k-1}{2} M^2 \right) \right]^{\frac{k+1}{2(k-1)}} \quad (\text{Eq. 3})$$

$$\frac{\rho_0}{\rho} = \left(1 + \frac{k}{2} M^2 \right)^{\frac{1}{k-1}} \quad (\text{Eq. 4})$$

$$M = \frac{V_g}{\sqrt{kRT_g}} \quad (\text{Eq. 5})$$

$$P_0 = \rho_0 RT_0 \quad (\text{Eq.6})$$

where, k : ratio of specific heat, R : gas constant, T_g : local gas temperature, T_0 : stagnation gas temperature, ρ_0 : stagnation gas density, ρ : local gas density, P_0 : stagnation gas pressure, A^* : critical area, M : mach number

Based on the above analysis, a novel high pressure HVOF torch with combustion chamber pressure up to 3.0 MPa was developed. This chamber pressure is higher than the most commercial industry available HVOF systems, which commonly operated below 1.0 MPa. Kerosene was used as fuel.

Particle temperature was controlled by lowering the flame jet temperature in this study. Different from injecting additional nitrogen gas or water into the combustion chamber, in this study, the flame jet temperature is controlled by adjusting the oxygen/fuel (O/F) ratio. Here we defined the normalized O/F ratio as variable λ in Eq.7.

$$\lambda = \frac{O_2 \text{ mole}}{Fuel \text{ mole}} / 19.35 \quad (\text{Eq. 7})$$

where, $O_2 \text{ mole}$ is the mole quantity of the oxygen gas, $Fuel \text{ mole}$ is the mole quantity of kerosene, and 19.35 is the stoichiometric flow ratio of kerosene

Therefore, $\lambda > 1$ corresponds to overstoichiometric conditions, indicating that excess oxygen gas flow was injected into the chamber. Thermal expansion of the unreacted free oxygen gas will exhaust reaction heat energy which results a drop in the flame jet temperature. Thus, the flame jet temperature can be controlled by varying λ . Higher λ results in lower flame temperature and consequently lower particle temperature.

Therefore, theoretically the particle velocity and temperature can be controlled by varying the chamber pressure and λ .

2.2 Experiment materials and process

The spray material used in the experiment was commercially available stainless steel 316L powder with nominal size range of $-44 +16 \mu\text{m}$ (Micro-melt® 316L). The powder presents a spherical morphology (Fig. 1). A stainless steel 304 sheet with size of 50 x 50 x 3 mm was used as a substrate. The deposition efficiency was measured by calculating the ratio between the mass of sprayed powder and the deposited mass onto the steel cylinders with a diameter of 260mm. Prior to spraying, the substrate was sandblasted with #36 brown fused alumina grits. In these studies, the stainless steel 316L particle velocity was measured by the DPV-2000 system under chamber pressures from 1.0 to 3.0MPa. The influence of λ and spray distance on deposition efficiency, microstructure and microhardness of the coating were investigated. A comparison to the JP-5000 system was also deduced.

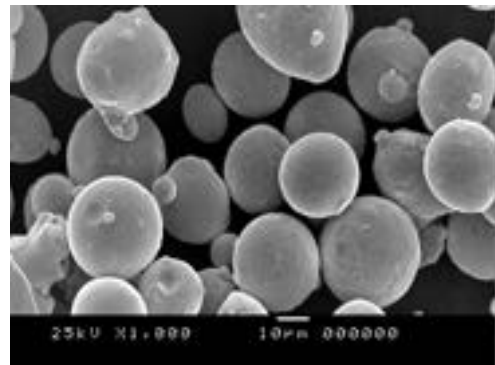


Fig. 1. Morphology of Micro-melt stainless steel 316L.

3 Experiment results

3.1 Particle Velocity

The influence of chamber pressure, λ and spray distance on the particle velocity were shown in Fig. 2, Fig. 3 and Fig. 4 respectively. The particle velocities were measured at a stand-off distance of 380mm from the nozzle exit. Under high pressure HVOF

conditions, the particle temperature can not be measured by the DPV-2000 system due to the low particle radiation intensity.

The influence of combustion chamber pressure on the particle velocity is shown in Fig. 2. The measurement was conducted at $\lambda = 2.0$. With the increase of chamber pressure from 1.0 to 2.0MPa, average particle velocity increased greatly from 430 to 640m/s, which is higher than that of the JP-5000 550m/s. With the further increase of chamber pressure to 3.0MPa the particle velocity increased slightly to 675 m/s. The measurement results indicated that improvements to particle velocity by higher chamber pressure are available.

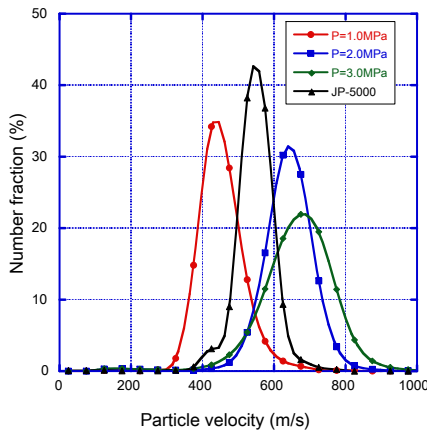


Fig. 2. Particle velocity distribution as a function of chamber pressure ($\lambda = 2.0$)

The influence of λ on the particle velocity was measured at a chamber pressure of 1.0MPa as shown in Fig. 3. Compared to the chamber pressure, λ exerts no significant influence on the particle velocity.

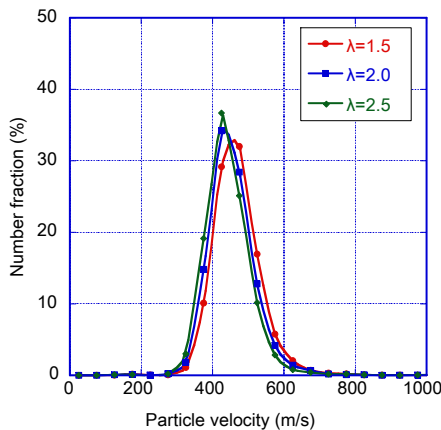


Fig. 3. Particle velocity distribution as a function of λ ($P = 1.0\text{MPa}$)

Fig. 4 shows the particle average velocity as a function of spray distance at a chamber pressure of 3.0 Mpa and $\lambda = 2.0$. The particle velocity increased from 705 to 730 m/s when the spray distance

increased from 100 to 200mm, and decreased with the further increase of spray distance to 380 mm.

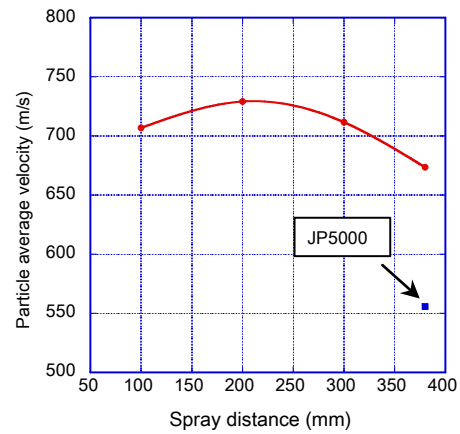


Fig. 4. Particle velocity as a function of spray distance ($\lambda = 2.0$, $P = 3.0\text{MPa}$)

3.2 Deposition efficiency

In the thermal spray process, the spray distance should be adjusted according to the type of spray process, power, spray materials, substrate and desired coating performance etc. Observation of the high pressure HVOF flame jet shows that the flame temperature may turn out to be quite lower with the increase of the λ . The flame jet may exert less oxidation or distortion effect on the substrate or deposited coatings. To investigate the effect of spray distance, a wide spray distance range from 50 to 300 mm was adopted to deposit coatings at the chamber pressure of 3.0MPa. Fig. 5 shows the deposition efficiency as a function of the spray distance at different λ .

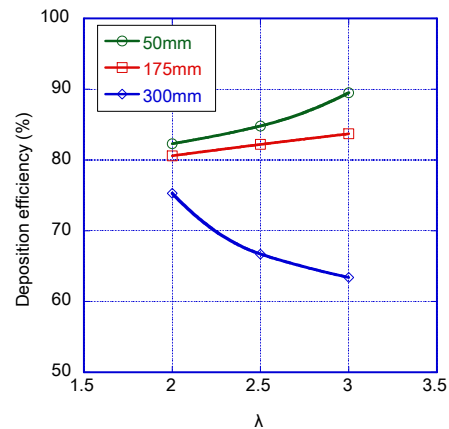


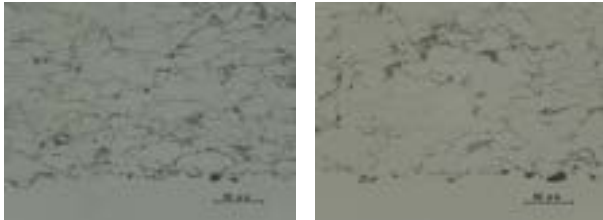
Fig. 5. Deposition efficiency ($P = 3.0\text{MPa}$)

At the short spray distance of 50 and 175mm, the deposition efficiency increased with the λ and reached a maximum of 90% at the spray distance of 50mm. It is higher than that of the JP-5000 and is approximate to the up-to-date cold spray process [17].

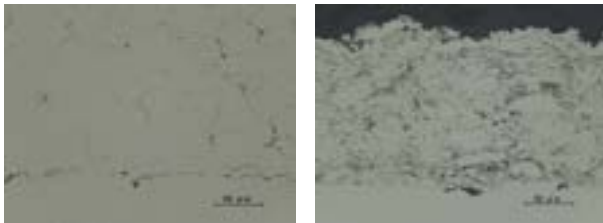
However, the deposition efficiency presents a decreasing trend as a function of λ at the spray distance of 300 mm.

3.3 Microstructure and microhardness

The typical microstructure of JP-5000 and high pressure HVOF sprayed stainless steel 316L coatings are shown in **Fig. 6**. The λ increased from 1.0 to 3.0 under the chamber pressure of 3.0MPa at the spray distance of 50mm. As an exception, the spray distance was set at 300 mm when $\lambda=1.0$ to prevent the substrate from overheating due to the flame jet.



(a) $\lambda = 1.0$, P = 3.0MPa spray distance = 300mm (b) $\lambda = 2.0$, P = 3.0MPa spray distance = 50mm

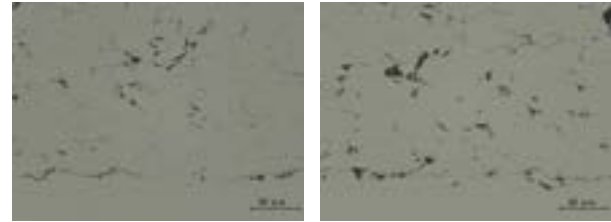


(c) $\lambda = 3.0$, P = 3.0MPa spray distance = 50mm (d) JP-5000 spray distance = 380mm

Fig.6 Microstructure of the stainless steel 316L coatings at different λ

At $\lambda=1.0$ (**Fig.6a**), the coating shows a near lamellar structure indicate that the spray powders experienced partial melting during spraying. The dark thin lamellae between the particles are oxides. At $\lambda = 2.0$ (**Fig.6b**), the particle deformation extent shows no significant change compared to $\lambda = 1.0$. However, the oxidation inclusions between the interfaces of the particle comparatively decreased. At $\lambda = 3.0$ (**Fig.6c**), except for few fine pores at the interface of adjacent particles, there are no visible oxidation inclusions in the coating that can be observed. It is noticeable that the particles deformation extent at $\lambda = 3.0$ is much less than that of $\lambda = 1.0$ or 2.0. The JP-5000 sprayed coating is composed of well deformed particles and it shows typical lamellar structure (**Fig.6d**). Massive oxidation inclusions indicate that the spray particles experienced were well molten during spray process. The coating microstructures sprayed at different spray distances are shown in **Fig. 7**. Comparing the microstructure of **Fig.6b** / **Fig.7a** and **Fig.6c** / **Fig.7b** deposited at different spray distance, it can be found that visible pores appeared between particle interface

at the spray distance of 300mm in both $\lambda=2.0$ and 3.0. It is noticeable that compared to the **Fig. 6b**, the **Fig. 7a** shows less oxidation in the coating. It can be deduced that the oxidation appearing in **Fig. 6b** occurred after the particle impacted on the substrate due to the short spray distance, as opposed to in-flight oxidation. Effective controlling of the substrate temperature during spraying may improve or eliminate the oxidation in the coating.



(a) $\lambda = 2.0$, P = 3.0MPa spray distance = 300mm (a) $\lambda = 3.0$, P = 3.0MPa spray distance = 300mm

Fig.7 Microstructure of the stainless steel 316L coatings at different spray distances

The microhardness of the coatings as a function of λ is shown in **Fig. 8**. The coatings microhardness decreased slightly with the λ and reduction in spray distance was benefit to obtain higher coating microhardness. The JP-5000 sprayed coating has a microhardness of 445.

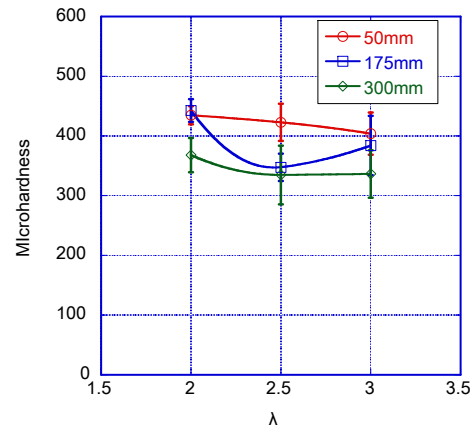


Fig.8 Coatings microhardness

4 Discussions

4.1 Particle velocity

The particle velocity measurement results showed that combustion chamber pressure exerts significant influence on the particle velocity (**Fig. 2**). The stainless steel 316L particle velocity of 675 m/s at the chamber pressure of 3.0MPa is comparable or even higher than that of the cold spray process [16]. Compared to chamber pressure, the λ gives no significant influence on particle velocity at a chamber

pressure of 1.0 MPa (**Fig. 3**). Theoretically, reducing λ will improve the particle velocity due to the higher flame jet velocity. However, the combustion products flow also decreased meanwhile with the reducing of λ , which results in lower gas density and consequently lower particle velocity. The independence of particle velocity to λ provided a feasible solution to independently control the particle velocity and temperature by merely varying the chamber pressure and λ . This method is more convenient and economic compared to adjusting the powder injection location [18].

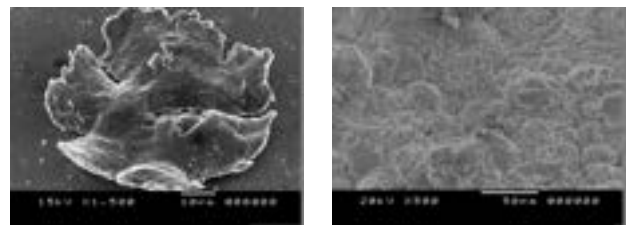
Short spray distance leads to improved deposition efficiency in the high pressure HVOF process as shown in **Fig. 8**. For example, 90%, 84% and 63% at the spray distance 50, 175 and 300mm respectively when $\lambda = 3.0$. However, examining the particle velocity it can be found that the particle velocity at spray distance of 50 mm is lower than that at 175mm. Therefore, the low deposition efficiency at long spray distance can be attributed to the cooling effect to the spray particle because the lowering of particle temperature results in an increase in the critical velocity. At the same time, it can be found that when the $\lambda = 3.0$, it exerts more significant influence on the deposition efficiency than $\lambda = 1.0$ and 2.0. Since the higher λ corresponds to the lower particle temperature, this experimental result is in accordance with the cold spray process, which is commonly operated at the short spray distance less than 50mm. The deposition efficiency at the spray distance of 50 and 175mm increased slightly with the λ . The reason is not clear but may be related to the particle oxidation film destruction during impact.

4.2 Microstructure and properties

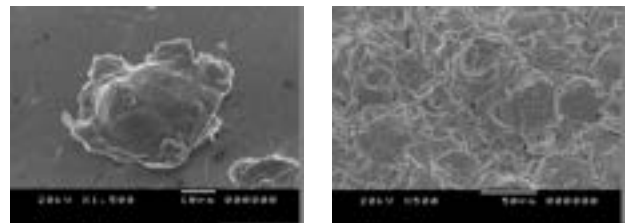
High pressure HVOF and JP-5000 sprayed stainless steel 316L coatings present different microstructure as shown in **Fig. 6**. The particle velocity measurement results and the coating microstructures reveal that particle velocity is the key factor in forming dense coatings. Although the particle temperature can not be measured in this studies, it is helpful to understand the particle melting state by observing the particle splat and coating surface morphology, as shown in **Fig. 9**. At $\lambda = 1.0$ (**Fig. 9a**), the unmolten splat shows sufficient plastic deformation and the coating is composed of a mixture of partially molten and molten particle. It should indicate that a few numbers of molten or partially molten splats could be observed in the low magnification microphoto at $\lambda = 1.0$. We can deduce that quite a number of particles have reached molten or partially molten state during in-flight at $\lambda = 1.0$. The splat deformation degree decreased when the λ increased over 2.0 and the coatings were completely composed of unmolten particles as shown in **Fig. 9b and Fig. 9c**. Compared to $\lambda = 3.0$, the coating presents a more dense microstructure when

$\lambda = 2.0$. Correspondingly, the coating microhardness at $\lambda = 2.0$ is slightly higher than that of $\lambda = 3.0$ (**Fig. 8**). Compared to the cold spray, high pressure HVOF shows the ability to the heat particles to include a wide range of melting states. As for the JP-5000 (**Fig. 9d**), the splat and coating surface morphology indicate that the spray particles experienced a completely molten state during spraying.

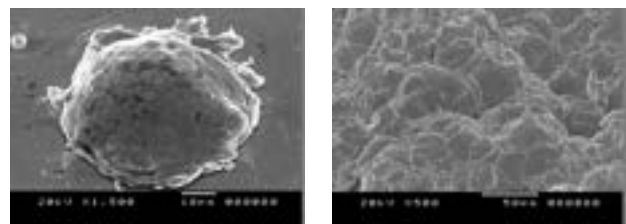
Other than λ , spray distance also influences on the microstructure and microhardness of the coatings. Coatings deposited at short spray distance trends to obtain higher microhardness and denser microstructure. These influences may be attributed to the cooling and deceleration effect on the particles due to the penetration of air into the flame jet [19].



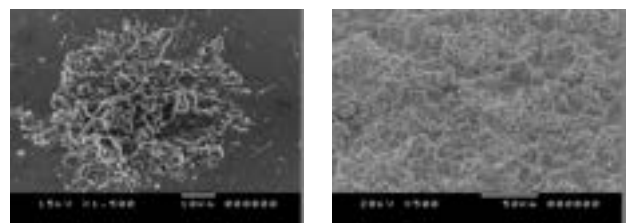
(a) $\lambda = 1.0$ spray distance: 300 mm P = 3.0 MPa



(b) $\lambda = 2.0$ spray distance: 50 mm P = 3.0 MPa



(c) $\lambda = 3.0$ spray distance: 50 mm P = 3.0 MPa



(d) JP-5000

Fig. 9 Splat and coating surface morphology

5 Conclusions

A high pressure HVOF system with combustion chamber pressure up to 3.0MPa, and with characteristics of higher flame velocity and lower

temperature was developed. Chamber pressure exerts significant influence on the particle velocity. The stainless steel 316L powders average velocity reaches 675m/s at the chamber pressure of 3.0MPa. The λ is the key factor in determining the particle melting state. The λ and the spray distance have significant influence on the microstructure, deposition efficiency and microstructure of the coatings. Dense coatings composed of unmolten or partially molten particles can be deposited at different spray parameters. This process can also be expected to deposit high-performance carbide-based cermet, metal and other alloy coatings.

6 Literature

- [1] C. Reignier, A. Sturgeon, D. Lee and D. De Wet: HVOF sprayed WC-Co-Cr as a generic coating type for replacement of hard chrome plating. International Thermal Spray Conference, Herausgeber, Essen, 2002, CD
- [2] T. Sahraoui, N-E. Fenineche, G. Montavon and C. Coddet: Alternative to chromium: characteristics and wear behavior of HVOF coatings for gas turbine shafts repair (heavy-duty). Journal of Materials Processing Technology, 152 (2004), pp. 43/55
- [3] C. J. Li, W. Y. Li: Effect of sprayed powder particle size on the oxidation behavior of MCrAlY materials during high velocity oxygen-fuel deposition. Surface and Coatings Technology, pp. 162 (2002), 31/41
- [4] L. D. Zhao, M. Parco and E. Lugscheider: High velocity oxy-fuel thermal spraying of a NiCoCrAlY alloy. Surface and Coatings Technology, 179 (2004), pp. 272/78
- [5] J. Kawakita, T. Fukushima, S. Kuroda, T. Kodama: Corrosion behaviour of HVOF sprayed SUS316L stainless steel in seawater. Corrosion Science, 44 (2002), pp. 2561/81
- [6] C. J. Li, A. ohmori, Y. Harada: Formation of an amorphous phase in thermally spray WC-Co, Journal of Thermal Spray Technology, 51 (1996), pp. 69/73
- [7] Y. F. Qiao, T. E. Fischer, A. Dentb: The effects of fuel chemistry and feedstock powder structure on the mechanical and tribological properties of HVOF thermal-sprayed WC-Co coatings with very fine structures. Surface and Coatings technology, 172 (2003), pp. 24/41
- [8] C. J. Li, H. Yang, H. Li: Effect of gas conditions on HVOF flame and properties of WC-Co coatings. Materials and Manufacturing Process, 14 (1999), pp. 383/95
- [9] A. Dolatabadi, V. Pershin, J. mostaghimi: New attachment for controlling gas flow in the HVOF process. Journal of Thermal Spray, 14 (2005), pp. 91/99
- [10] S. Krudo, J. Kawakita, M. Watanabe, H. Katanoda: Warm spraying – a novel coating process based on high-velocity impact of solid particles. Science and Technology of Advanced Materials. 9

(2008), pp. 1/17

- [11] R. Dhiman, F. Farhadi, L. Pershin, S. Chandra, J. Mostaghimi: Development of a low-temperature (LTOF) thermal spray gun. International Thermal Spray Conference, Singapore, 2010, CD
- [12] A. Wank, A. Schwenk, M. Liu, K. S. Zhou, C.M. Deng and C. G. Deng: Expansion of the applicable range of HVOF process conditions. International Thermal Spray Conference, Singapore, 2010, CD
- [13] J. kawakita, S. Kuroda, T. Fukushima, H. karanoda: Dense titanium coatings by modified HVOF spraying. Surface & Coatings Technology, 201 (2006), pp. 1250/55
- [14] M. Grujicic, J. R. Saylor, D. E. Beasley, W. S. DeRosset, D. Helfritsch: Computational analysis of the interfacial bonding between feed-powder particles and the substrate in the cold-gas dynamic-spray process. Applied Surface Science, 219 (2003), pp. 211/27
- [15] H. Fukanuma, N. Ohno, B. Sun, R. Z. Huang: In-flight particle velocity measurements with DPV-2000 in cold spray. Surface & Coatings Technology, 201 (2006), pp. 1935/41
- [16] T. Stolenhoff, H. kreye, H.J. Richter: An analysis of the cold spray process and its applications. Journal of Thermal Technology, 11 (2002), pp. 542/50
- [17] H. Fukanuma, R. Huang: Development of high temperature gas heater in the cold spray coating system, International Thermal Spray Conference, 2009, Las Vegas, pp. 267/72
- [18] T. C. Hanson, C. M. Hackett, G. S. Settles: Independent control of HVOF particle velocity and temperature. Journal of Thermal Spray Technology, 11 (2002), pp. 75/75
- [19] K. Dobler, H. Kreye, R. Schwetzke: Oxidation of stainless steel in the high velocity oxy-fuel process. Journal of Thermal Spray Technology, 9 (2000), pp. 407/13